

Review

Dirac Cones in Graphene, Interlayer Interaction in Layered Materials, and the Band Gap in MoS₂

Ivan N. Yakovkin

Institute of Physics of National Academy of Sciences of Ukraine, Prospect Nauki 46, Kiev 03028, Ukraine; yakov@iop.kiev.ua or i.n.yakovkin@gmail.com

Academic Editors: Cristina E. Giusca and Spyros Yannopoulos

Received: 15 June 2016; Accepted: 4 November 2016; Published: 10 November 2016

Abstract: The 2D outlook of graphene and similar layers has initiated a number of theoretical considerations of electronic structure that are both interesting and exciting, but applying these ideas to real layered systems, in terms of a model 2D system, must be done with extreme care. In the present review, we will discuss the applicability of the 2D concept with examples of peculiarities of electronic structures and interactions in particular layered systems: (i) Dirac points and cones in graphene; (ii) van der Waals interaction between MoS₂ monolayers; and (iii) the issue of a 2D screening in estimates of the band gap for MoS₂ monolayers.

Keywords: atomic layers; 2D systems; MoS₂; graphene; Dirac cone; electronic structure; band gap; DFT calculations; interlayer interaction; 2D screening

1. Introduction

Layered systems have special properties which make them very promising in various applications such as nanoelectronics and catalysis [1–8]. The variety of graphene-like atomic layers can now be synthesized by means of the liquid exfoliation technique, which provides opportunities for systematically tailoring the surface properties [1,9]. In electronic applications of the layered systems, one of the most important issues is the width of the band gap, which is absent in graphene. The metallicity is usually inappropriate for application, and a number of recent studies has been devoted to the band structures of graphene nanoribbons, where the gap opens because of the spatial restrictions. A great interest in the MoS₂, a typical representative of layered transition metal dichalcogenides, has been roused not only by its well-known lubrication properties but also by its very suitable band gap width (about 1 eV) for applications in nanoelectronics [10].

Several transition-metal dichalcogenides exhibit the transformation from indirect to direct band gap semiconductors as they are thinned down to a single monolayer. For example, a MoS₂ monolayer exhibits a dramatic increase in luminescence quantum efficiency compared to the bulk material [11,12]. The explanation for these phenomena was found with the help of the band structure calculations [12–16], which have revealed the transformation of the band gap from an indirect one for the bulk MoS₂ to a direct one for the monolayer and an increase in the width of the band gap.

It is well established that DFT underestimates band gaps and, for bulk band structures of semiconductors and insulators, much better values in general can be obtained using the quasiparticle approach in *GW* approximation suggested by Hedin [17]. This method provides an estimate of the self-energy operator (seen from the perspective of electron density) by using Green's function *G* for the electron system, in the screened Coulomb field *W*. Parameters of screening and inverse dielectric function are obtained with solutions of Kohn-Sham (KS) equations, which allow the estimation of many-body corrections to the KS bands. The great success of *GW* in various applications for semiconductors ultimately proves its usefulness and validity for bulk calculations. However, in the 2D (2-dimensional) case, the screening dramatically differs from the screening in a bulk, so that the

validity of the dielectric function in 2D systems is not obvious, as discussed in the present review paper and illustrated by examples of calculations of the band structure of free MoS₂ monolayers.

One of the most exotic—and generally accepted—theories is the existence of relativistic effects in graphene, leading, in particular, to the emergence of the Dirac cones in the electronic structure (see, e.g., [2–6] for reviews). The band structure of graphene in vicinity of the K point can be depicted with the help of conical surfaces—the Dirac cones—similar to light cones, which makes the analogy with photons even more transparent. Consequently, it was concluded that electrons at the K point also must be zero mass particles, that is, become massless Fermions instead of usual quasiparticles in solids. As such, they obviously could not be treated by Schrödinger's equation and therefore require the Dirac theory. There is a great number of theoretical papers devoted to applications of the Dirac theory to graphene-containing layered systems (for review, see, e.g., [2–6]). A powerful technique of quantum electrodynamics and group theory has provided a detailed explanation of the peculiarities of the graphene electronic structure. It should be mentioned, however, that the linear dispersion and E_F band crossing at the K point were obtained from band structure calculations performed with one or another form of Schrödinger's equation (for example, within DFT or tight-binding approximation), which afterwards were suggested to be invalid.

In the following sections, we will discuss the applicability of the 2D concept with examples of peculiarities of electronic structures and interactions in particular layered systems: (i) Dirac points and cones in graphene (Section 2); (ii) van der Waals interaction between MoS₂ monolayers (Section 3); (iii) screening and estimates of the band gap for MoS₂ monolayer (Section 3). The band structures of model layered systems, distributions of electronic densities, and interlayer interactions, presented in Figures 1–4, were calculated with the ABINIT program package, using the supercell model, norm-conserving pseudopotentials, and LDA approximation for exchange-correlation; see [15] for details. Main conclusions and final remarks are presented in Section 4.

2. Dirac Cones and Buckling in Graphene and Similar Layers

The band structure of graphene indeed has a quite unusual feature—the crossing of the Fermi level at the K point of the Brillouin zone (the Dirac point) by bands with a linear dispersion relation, thus forming Dirac cones (Figure 1a). As mentioned above, the zero-gap property of graphite and graphene restricts the area of their applications. For this reason, there is considerable activity in search of ways to open and control the band gap in graphene. Several methods have been proposed, in particular (i) adsorption interaction with the substrate and intercalation [7,18,19]; (ii) lattice distortion causing the symmetry reduction [2,3,20–24]; and (iii) structural confinements (such as in nanoribbons and islands) [25,26]. The produced band gaps were observed in photoemission experiments (in particular, with help of the modern real-time band mapping technique), and thus were considered to prove the Dirac theory due to the observations of cone-like bands. It should also be mentioned that adsorption or intercalation of alkalis results in *n*-doping of graphene layers and related shift of the Fermi level [27,28], so that the cone bands occur well below E_F. Similar shifts of the bands were reported as a result of the interaction of graphene monolayers with the substrate surface [7,19,29–32]. For example, it was found, by angle-resolved photoelectron spectroscopy, that graphene on Ir(111) displays a Dirac cone with the Dirac point shifted only slightly above the Fermi level. The moiré resulting from the overlaid graphene and Ir(111) surface lattices imposes a superperiodic potential giving rise to Dirac cone replicas and the opening of minigaps in the band structure [33].

Sante et al. [34] studied a more general case of the emergence of ferroelectricity in two-dimensional honeycomb binary compounds and demonstrated the important role of a metal substrate in induced buckling. In particular, it was found that the buckled structure of two-dimensional AB binary monolayers is inherent for honeycomb lattice with trigonal symmetry, so that arising dipoles can lead to ferroelectricity.

Now, again, let us consider the 2D concept of graphene in more detail. First of all, a perfect free standing infinite monolayer is only a model, which, while very useful, has inherent restrictions, which

should be kept in mind when applying the theory to real systems. Even when the interaction with the substrate is substantially diminished, it is nonetheless present and thus unavoidably affects the peculiarities of the electronic structure such as Dirac cones.

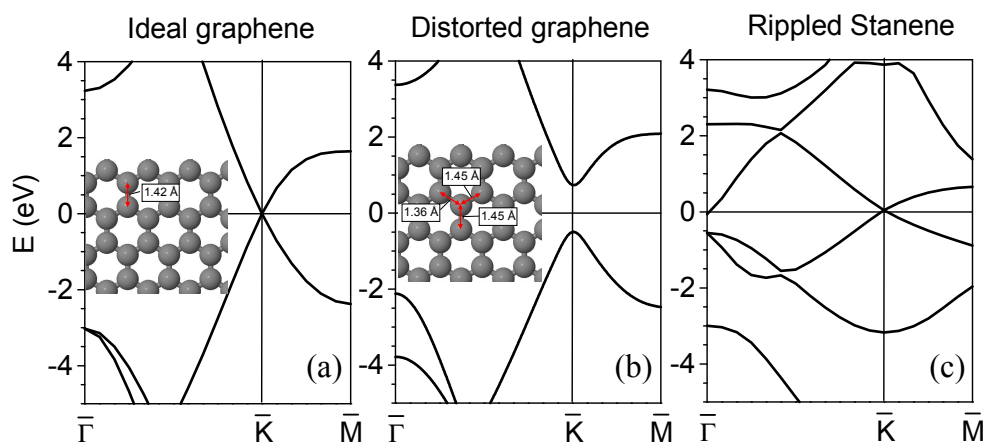


Figure 1. Band structures in vicinity of Fermi level for (a) an ideal free graphene; (b) distorted graphene monolayer; and (c) rippled Sn monolayer (stanene).

Rigorously speaking, single graphene layers cannot exist in a freestanding form, because strictly 2D crystals are thermodynamically unstable [35,36]. Specifically, a divergent contribution of thermal fluctuations in low-dimensional crystal lattices should lead to displacements of atoms that are comparable to interatomic distances at any finite temperature. Using first-principles calculations of graphene with high-symmetry distortion or defects, Lee et al. [37] investigated band gap opening through chiral symmetry breaking in graphene. It was shown that the Peierls distortion takes place in biaxially strained graphene, leading to structural failure. The chiral symmetry breaking in honeycomb lattices was demonstrated to be responsible for the gap opening in graphene antidotes [2] and armchair nanoribbons [38]. Similar conclusions were derived from the theoretical study of Peierls-type instability in functionalized graphene [39]. In particular, it was shown that Bragg scattering of electron waves induced by sublattice symmetry breaking results in a band gap opening, whereby Dirac fermions acquire a finite mass.

The reduction of symmetry from C_{6v} to C_{3v} , by breaking the equivalency of the graphene sites, leads to the opening of a band gap in the otherwise gapless semiconductor graphene [23]. It should be noted that there is an interplay between the energy cost or strain energy for graphene structural reconstructions and reduction in energy opening up a band gap, but when a reduction of the symmetry is allowed, graphene can lower the total free energy of the system and a band gap will open at the Dirac point. The opening of the gap due to the layer distortion can be illustrated by means of calculations for a model distorted graphene layer, in which every second atom is shifted by ~ 0.05 Å in the direction towards one of the 3 nearest neighbors (as depicted in the insert in Figure 1b). This type of distortion indeed results in the opening of the band gap (Figure 1b), as anticipated.

If the displacement of carbon atoms is performed normal to the layer (that is, in the z direction), the generated forces tend to return the layer to a plain configuration. This behavior is inherent just for graphene, while, for example, a free honeycomb Sn monolayer (stanene) spontaneously reconstructs forming a rippled structure with the vertical corrugation of 0.7 Å. The rippled structure is favored with respect to the flat (plain) structure of stanene by 0.2 eV. However, the corrugation does not open the band gap (Figure 1c). The explanation can be found in the theory of Peierls transitions. In particular, it was suggested that a transversal distortion does not lift degeneracy at the Brillouin zone edge and hence does not lead to the opening of the band gap [40]. This statement was illustrated by the example

of the non-metal to metal transitions in atomic wires [41,42], and is probably also valid for 2D metallic layers, as may be concluded from a metallic state of the rippled Sn monolayer.

It should be noted in this regard that the corrugation is typical for graphene layers adsorbed on various surfaces, which is evident, for example, for graphene on Ir(111) from the forming moiré patterns resulting from the overlaid of graphene and substrate surface lattices [33]. Another typical example is a single-layer graphene on the Ru(0001) surface, which forms hexagonal superstructures [18,29] related to ordered structures of humps on overall flat graphene layers. Because of the metal substrate, it is difficult to conclude whether the state of the adsorbed graphene might be characterized as semiconducting in these and similar adsorption systems.

The role of the structure and interlayer interaction can be better understood by using the model of a free graphene bilayer. In a bulk graphite, every second layer is shifted—so that in the unit cell, one atom of the second layer is atop the atom of the first layer while the other occurs above the hole of the honeycomb cell. The same structure (the AB configuration of the layers), with a distance between the layers of 3.30 Å, is found to be favorable also for the bilayer graphene. The structure with symmetric position of the layers with respect to the xy plane (that is, AA) is only slightly (by 0.014 eV) less favorable than the original shifted (AB) structure, which indicates a possibility of its formation under certain external influence (e.g., impurities or temperature fluctuations).

The bilayer with shifted graphene layers (AB) is metallic (Figure 2a), though DOS at E_F is small. For graphene layers, symmetric with respect to the $z = 0$ plane (AA), in contrast, the bilayer becomes a semiconductor with the direct gap of 0.45 eV (Figure 2b). It should be noted that the drastic change of the electronic structure from semimetal to semiconductor caused by the relative shift of graphene monolayers indicates an importance of the interlayer interaction in graphite and raises the question of whether this interaction is indeed vdW in nature.

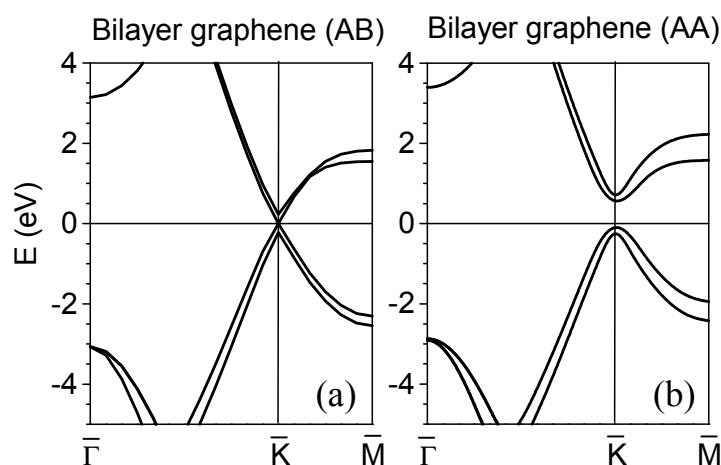


Figure 2. Band structures for free graphene bilayers with the AB layer configuration, pertinent to a bulk graphite (a); and the AA configuration, in which carbon atoms of the second layer are positioned atop the atoms of the first layer (b).

In summary, in one-dimensional metallic systems the electron-phonon interaction leads to the Peierls instability. The same is valid also for 2D systems, so that an ideal 2D crystal is unstable with respect to various possible lattice distortions leading to the opening of the band gap at E_F , that is, to a semiconducting state of the layer.

It should be emphasized that the instability of 2D system is inherent and will unavoidably cause the distortion of the structure of a free graphene monolayer. Then, the Peierls distortion will cause the opening of the band gap, which means that the Dirac cone in graphene in reality will transform into ordinary band vertex. Indeed, regardless the cause of opening the band gap or the shift of the bands, the cone-like bands are no longer perfect cones and therefore do not need any

relativistic description. This conclusion directly follows from a great number of experimental and theoretical results obtained for graphene containing layered systems. A few examples of photoemission studies and related conclusions: (i) Bragg scattering of electron waves induced by sublattice symmetry breaking results in a band gap opening, “whereby Dirac fermions acquire a finite mass” [39]; (ii) there is a quasiparticle transformation during a metal–insulator transition in graphene [43]; (iii) observation, both in angle-resolved photoemission and theory, of a mismatch between the upper and lower halves of the Dirac cone [44]; and (iv) the Peierls-like distortion, destroying the Dirac point of graphene and opening a substantial energy gap, was reported for graphene on SiC [45].

Carbon is number 6 on the periodic table, and its core charge is too small to give rise to any significant relativistic effects. This is obvious, and the only reason to consider the Dirac theory comes from the special perfect cone shape of the bands crossing E_F at K point, which, nonetheless, can be calculated without involving the Dirac equations, for a free perfect infinite graphene monolayer. In reality, however, a free perfect monolayer never can be obtained, and therefore the perfect cone bands at K point of BZ for graphene, as follows also from all performed to-date photoemission experiments, can exist only in theory, while in reality the cone will unavoidably be distorted because of the related change of symmetry. In other words, the cone-like bands observed in photoemission experiments are *not* true Dirac cones, as they, in fact, do *not* correspond to zero-mass Fermions. This is good news, because it allows for ordinary non-relativistic DFT calculations for graphene-containing layered structures.

3. The Interlayer Interaction in Layered Crystals

The interlayer interaction in inherently layered crystals (graphite, MoS₂) is usually explained by van der Waals (vdW) forces. It should be clarified in this regard that physical chemistry attributes all interactions beyond Coulomb and exchange interactions to vdW forces, which therefore include electrostatic forces between permanent dipoles (Keesom forces), permanent dipoles and a corresponding induced dipoles (Debye forces), and London dispersion forces (which are sometimes explained in terms of the interaction between instantaneously induced dipoles). The modern understanding of dispersion forces does not involve the concept of temporal virtual dipoles and explains the attraction between neutral molecules in terms of electrostatic forces. This type of interatomic interaction is of the same origin as the exchange interaction between electrons which can be explained as Coulomb interaction of fermions having antisymmetric wave functions. In solid state physics, it is usually just the dispersion forces that are called van der Waals forces.

The concept of dispersion forces appeared in 30-th of former century aiming an explanation of the attraction between neutral molecules at distances for which, as it was believed, a direct overlap of wave functions must be negligible [46,47]. Since the attraction between neutral species at relatively large distances, which seemingly preclude the overlap of wave functions, does exist, there must be a mechanism to accomplish this interaction. This might be the vdW interaction, as nothing better has been proposed, which is absent in standard DFT calculations using the local (LDA) and semilocal (GGA) approximations for exchange-correlation potentials [48,49].

It was proposed then to introduce some form of vdW term into the GGA functional to obtain vdW-corrected semilocal potentials, which correctly reproduce the asymptotic van der Waals tail of the binding energy curve [50–55], or even make use of truly non-local potentials developed with account for many-body interactions [56,57]. With any of these approximations, of course, significant improvements (with respect to GGA) of the estimates of interatomic and interlayer distances were achieved, which were considered therefore proving the validity of the vdW corrections.

However, the nonlocal corrections have little impact on the charge distribution at the graphene/metal interface [58,59], so that, for the graphene/metal systems, the vdW-DF results were found to be qualitatively similar to the LDA results [58]. This unexpected property of LDA is well known and has been usually attributed to a fortunate cancellation of errors in the exchange-correlation functional; nonetheless, the agreement of many LDA-calculated values with experiment is remarkable.

The LDA is known to provide, in many cases, better evaluation of the ground state properties (such as energies of occupied bands and electron density distribution) and estimates of binding energies in layered systems than widely used GGA [58–60]. For example, for graphene/Ir(111), GGA gives almost zero bonding, while LDA gives correct results both for binding energies and interatomic distances [58]). It should be mentioned also that LDA has a number of advantages with respect to GGA and other more sophisticated approximations, such as LDA+U, LDA+I, and LDA+vdW. Indeed, the f -sum rule is strictly fulfilled in LDA, but not in GGA, and for this reason GGA fails in description of Friedel oscillations.

Shulenburger et al. [61] performed quantum Monte Carlo calculations and found that the interlayer interaction in few-layer phosphorene is associated with a significant charge redistribution that is incompatible with purely dispersive forces. This result raises a question about the true nature of the interlayer interaction in so-called “van der Waals (vdW) solids”. It should be mentioned also that despite the revealed incapability of density functional theory calculations with different vdW corrected functionals to correctly capture the charge distribution, the LDA-calculated dependences of the interlayer interaction on the distance between the layers are in fairly good agreement with quantum Monte Carlo results, while GGA estimates are inconsistent.

The applicability of LDA to layered systems can be further illustrated by calculating the distribution of electronic density and related interlayer interaction for MoS₂ bilayer [15] (Figure 3). The most important result of the calculations is the revealed significant overlap of the wave functions of adjacent MoS₂ layers (the distribution of the plane-averaged electronic density of the bilayer along the normal to the surface is shown in Figure 3b). In contrast, the GGA gives a substantially different distribution of electronic density (shown by dashed line in Figure 3b). In particular, the GGA electronic density at the middle point between the layers is found to be approximately 10 times less than in LDA calculations. Accordingly, the energy of the interlayer interaction, estimated with GGA, decreases to 0.008 eV/cell from the LDA value of 0.12 eV/cell.

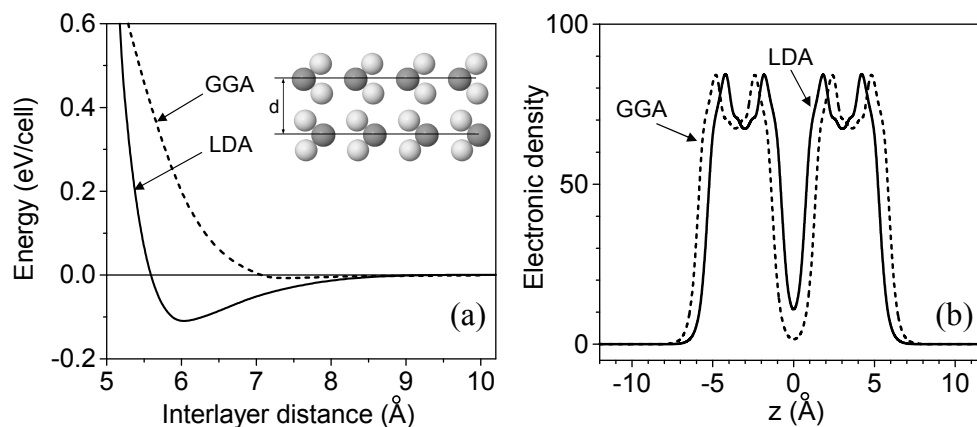


Figure 3. The dependence of the energy of interlayer interaction (per unit cell) for the MoS₂ bilayer on the distance between the layers (a) and the plane-averaged electronic density of the bilayer along the normal to the surface (b). LDA and GGA results are shown by solid and dashed lines, respectively.

It should be noted that dispersion forces, responsible for van der Waals interactions of non-polarized particles, were introduced to explain the attractive interaction which exists between neutral atoms and molecules when the overlap of the wave functions is seemingly negligible. Rigorously speaking, when the overlap is substantial, one cannot invoke the vdW interaction, but, rather, has to consider some type of the exchange or, in chemical terms, covalent interaction.

Hence, within LDA, there is no need to involve the London dispersion forces to explain the interaction, which, in fact, originates from the overlap of the wave functions of the layers, and therefore it is the exchange interaction that provides the bonding between the layers. The vdW

corrections to the exchange–correlation functional (or exploration of non-local functionals) [49–57] are mandatory when interlayer interactions are estimated within GGA, which dramatically underestimates the electronic densities of the electrons leaking from the surfaces to vacuum and thus the overlap of the wave functions of adjacent layers, while LDA itself is sufficient to adequately describe the interlayer interaction. This suggestion is further supported by a good agreement of calculated phonon frequencies at zero wave vector with experimental values [15].

The interlayer interaction in MoS₂ can be significantly increased by means of H or alkali metal intercalation. In particular, for hydrogen-intercalated MoS₂ bilayers, due to forming S–H–S bonds, the interaction energy increases from 0.12 eV to 0.60 eV [62]. Very similar results were also reported for Li [63] and Na [64] intercalated MoS₂ bilayers. However, in contrast to intercalated hydrogen, Li and Na do not reconstruct the MoS₂ bilayer, which retains the central symmetry pertinent to the bulk. In all cases, the intercalation leads to metallization, which is evident from the appearance of the bands crossing Fermi level and significant density of states at E_F.

There is one issue to be mentioned with regard to the interlayer or interatomic interaction—the repulsion between the layers or atoms that appears when the interatomic distance becomes less than the equilibrium distance. Usually this repulsive interaction—in particular, in most chemical papers—is called, perhaps for historical reasons, “Pauli repulsion”, thus implying its origin is the requirement that the Pauli principle be obeyed. In fact, the term indicates an exchange interaction, which exists at any distance between the atoms (or from an atom to the surface) simultaneously with Coulomb interactions (electron–core, core–core). Furthermore, the kinetic energy and correlation energy of electrons also must be taken into account to estimate the equilibrium interatomic distances. Fortunately, the DFT within LDA successfully solves this problem.

4. Band Gap and Screening in MoS₂ Layers

Fully relativistic (i.e., with account for a spin-orbit interaction) band structures of the bulk MoS₂ and free MoS₂ monolayer, calculated within LDA [15], are shown in Figure 4. The reduced symmetry of the monolayer (because of the absence of the inversion symmetry) with respect to the bulk MoS₂ reveals itself in the *k*-dependent spin-orbit splitting of the bands [65–69] (Rashba effect). At K point of BZ the splitting of the topmost valence band is quite pronounced (0.15 eV).

In contrast, for the bulk, because of Kramers degeneracy [$E_{\uparrow}(k) = E_{\downarrow}(k)$], originated from the combination of time-reversal [$E_{\uparrow}(k) = E_{\downarrow}(-k)$] and inversion symmetry [$E_{\uparrow}(k) = E_{\uparrow}(-k)$] [65,66], similar relativistic calculations have not indicated any spin-orbit splitting of the bands.

In agreement with recent experiments [11,12], the DFT calculations [13–16,70,71] demonstrate a transformation from indirect band gap for the bulk to direct band gap and its significant increase for the monolayer. However, while the DFT calculations, in general, correctly describe the evolution of the band structure, the width of the gap for the bulk is strongly underestimated. Specifically, for the bulk MoS₂, the LDA-estimated gap of 0.76 eV is significantly less than the experimental value 1.2–1.3 eV.

The underestimate of the band gaps in DFT calculations, in particular, within LDA, is well known (see [72] for a concise review). In bulk calculations of the band structures of semiconductors, as well as for layered systems with relatively small interlayer spacing, such as FeS₂, GGA, due to increased (by 10/7 [73]) exchange term in the PBE [74] exchange–correlation functional [72] usually gives somewhat better estimates of the gaps [75]. (It should be mentioned in this regard that GGA has severe intrinsic problems, in particular, the sum rule for the exchange–correlation hole cannot be satisfied, which leads to an incorrect behavior of the wave function, so that, for example, Friedel oscillations do not appear with the gradient corrections to LDA [61]; furthermore, the gradient expansion does not converge (that is, invalid) for any realistic systems, where the density gradients always exceed the convergence criterion for an order of magnitude [61,76,77]).

In contrast to the LDA results, the band gap for a bulk MoS₂, estimated in [14] using a sophisticated quasiparticle self-consistent GW approximation (QSGW), is found to be 1.297 eV, which is in a

perfect agreement with the generally accepted experimental value. For a MoS₂ monolayer, however, the gap calculated either with GW or QSGW approximation (2.759 eV [14]), exceeds the 1.90 eV energy of a prominent photoluminescence (PL) band by ~0.9 eV. To explain this dramatic difference, it was suggested [14] that the PL band originates from the recombination of a 2D Wannier–Mott exciton with enormously high binding energy because of inherently 2D screening of the Coulomb interaction in the monolayer.

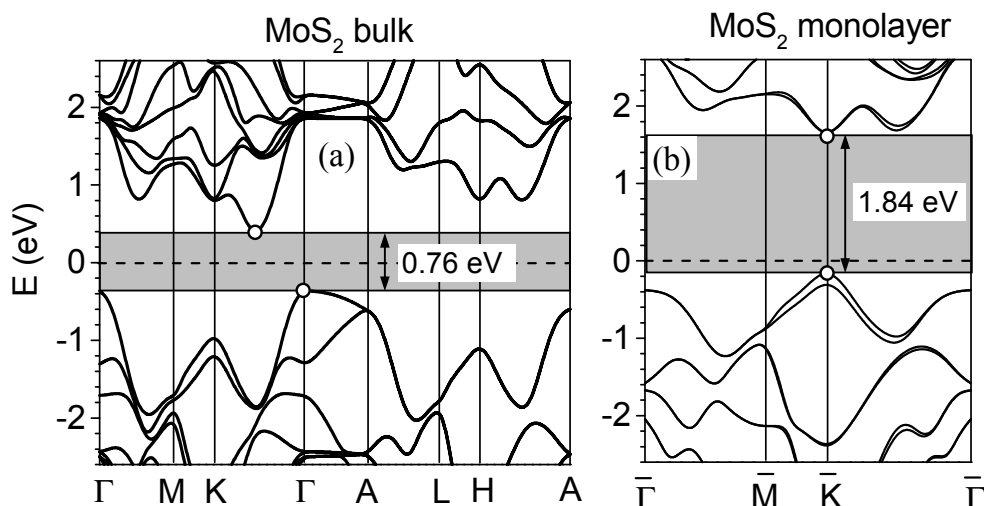


Figure 4. The band structures of the (a) bulk MoS₂ and (b) MoS₂ monolayer calculated within LDA in a fully relativistic (i.e., with account for spin-orbit coupling) approximation. Shaded areas denote the band gaps. Valence band maxima and conduction band minima are marked by circles.

Quasiparticle band structures and optical properties of MoS₂, MoSe₂, MoTe₂, WS₂, and WSe₂ monolayers were studied also using the GW approximation in conjunction with the Bethe–Salpeter equation [78]. The transition energies for monolayer MoS₂ are shown to be in excellent agreement with available absorption and photoluminescence measurements. Similar conclusions were derived also from the study of many-body effects and diversity of exciton states and their role in the formation of the optical spectrum of MoS₂ by Qiu et al. [79] and in recently performed STS and PL studies of MoSe₂ layers on graphene substrate, supported by GW and Bethe–Salpeter calculations of exciton binding energies [80,81]).

Because of excitons involved into the processes of luminescence and light absorption [82], the determination of the width of the band gap is not always straightforward. Furthermore, recently discovered trions [83–86] could further complicate the interpretation of the spectra. A more direct method of the determination of the “electronic” band gap (in contrast to “optical” band gap estimated from PL) could be the photoconductivity spectroscopy. In particular, for a MoS₂ monolayer, Mak et al. [11] reported an abrupt rise of photoconductivity by 3 orders of magnitude at ~1.8 eV, which was attributed to a direct gap photoexcitation. (It should be noted, however, that this value is lower than the energy of the PL peak, reported in this study, which is somewhat confusing and might be attributed to some influence of the substrate and conditions of the experiment).

Recent layer-specific direct measurements of band gaps of in MoS₂ and ReS₂ by high resolution electron energy loss spectroscopy (HREELS) [87] have reported an indirect band gap of 1.27 eV obtained from the multilayer regions (i.e., essentially bulk MoS₂). For the monolayer, the band gap becomes direct (with the valence band maximum and conduction band minimum at the K point of the Brillouin zone) and increases to 1.98 eV. For monolayer MoS₂, the twin excitons (1.8 and 1.95 eV) originating at the K point are observed (note the 0.15 eV exchange splitting due to Rashba effect, c.f. with the theoretically estimated splitting, Figure 4b). It should be noted that the energies of the exciton peaks determined by HREELS [87] well agree with the energies of PL lines for the MoS₂ monolayers [12].

Then, the difference between the width of the band gap for the monolayer (1.98 eV) and the energies of PL lines (1.8 and 1.95 eV) is about 0.03–0.18 eV, which is in reasonable agreement with anticipated (i.e., usual) values of Wannier-Mott exciton binding energies [82]. The energy of trion, which also was reported to be detected for the monolayer, is also in this range.

A number of recent papers was devoted to detailed studies of a model 2D heterostructure formed of a single layer of MoS₂ on graphene [88–93]. It was found that the electronic structure of two-dimensional (2D) semiconductors can be significantly altered by screening effects. The results obtained using time- and angle-resolved photoemission (ARPES) reveal a significant (~400 meV) reduction of the band gap of the MoS₂ layer induced by optical excitation [89]. The band gap and photoluminescence shift were reported to depend on the orientation of the graphene and MoS₂ monolayers [90,91]. The changes in electronic structure of graphene caused by interaction with MoS₂ monolayer were suggested to be less pronounced. From ARPES study of this heterostructure Diaz et al. [92] concluded that the Dirac cone of graphene remains intact and no significant charge transfer doping was detected. Later, Pierucci et al. [93] confirmed that, close to the Fermi level, graphene exhibits a robust, almost perfect, gapless Dirac cone, but suggested the graphene to be *n*-doped.

In summary, available experimental data suggest that the band gap in MoS₂ monolayer is in the range of 1.8–2.15 eV. Then, the 2.9 eV value obtained in GW calculations either should be attributed to the difference between “electronic” and “optical” gaps, produced by excitons with enormously large binding energies, or to apparent problems with evaluations of 2D dielectric function. In my view, the latter explanation is more consistent since it also explains the values obtained for the gaps in photoconductivity and HREELS measurements.

5. Conclusions

The 2D concept has reached its peak in the reanimation of Dirac theory applying to the band structure of graphene. Recall that carbon is number 6 in the periodic table, and its core charge is too small to give rise to any significant relativistic effects. This is obvious, and the only reason to consider the Dirac theory comes from the special perfect cone shape of the bands crossing E_F at the K point (which, nonetheless, can be calculated without involving the Dirac equations), for a free perfect infinite graphene monolayer. It is well known that a free perfect monolayer can never exist in reality because of an inherent instability, and therefore the perfect cone bands at the K point of BZ for graphene, as also follows from all performed to-date photoemission experiments, can exist only in theory, while in reality the cone will unavoidably become distorted because of the related change of symmetry. In other words, the cone-like bands observed in photoemission experiments are *not* true Dirac cones, as they, in fact, do *not* correspond to zero-mass Fermions. This is a good news, because allows for ordinary non-relativistic DFT calculations for graphene-containing layered structures.

Most likely, these statements seem too strong and not well enough argued, but, in fact, everybody faced with 1D and 2D concepts and related theories will find the conclusions correct (recall also that the real World is 3D). That is, though everybody feels that relativistic effects in coil (or graphene) are hardly likely to occur, nobody has been brave enough to say this publicly. Now I, like the little boy from Andersen's tale, have said: “But the Emperor has nothing at all on!”.

Conflicts of Interest: The authors declare no conflict of interest.

Abbreviations

The following abbreviations are used in this manuscript:

DFT	Density Functional Theory
LDA	Local Density Approximation
GGA	Generalized Gradient Approximation
GW	GW quasi-particle Hedin's approach
QSGW	Quasiparticle Self-consistent GW approximation

BZ	Brillouin Zone
vdW	van der Waals
HREELS	High Resolution Electron Energy Loss Spectroscopy
2D	2-Dimensional

References

- Novoselov, K.S.; Jiang, D.; Schedin, F.; Booth, T.J.; Khotkevich, V.V.; Morozov, S.V.; Geim, A.K. Two-dimensional atomic crystals. *Proc. Natl. Acad. Sci. USA* **2005**, *102*, 10451–10453. [[CrossRef](#)] [[PubMed](#)]
- Geim, A.K.; Novoselov, K.S. The rise of graphene. *Nat. Mater.* **2007**, *6*, 183–191. [[CrossRef](#)] [[PubMed](#)]
- Geim, A.K. Graphene: Status and Prospects. *Science* **2009**, *324*, 1530–1534. [[CrossRef](#)] [[PubMed](#)]
- Castro Neto, A.H.; Guinea, F.; Peres, N.M.R.; Novoselov, K.S.; Geim, A.K. The electronic properties of graphene. *Rev. Mod. Phys.* **2009**, *81*, 109. [[CrossRef](#)]
- Novoselov, K.S.; McCann, E.; Morosov, S.V.; Fal'ko, V.I.; Katsnelson, M.I.; Zeitler, U.; Jiang, D.; Schedin, F.; Geim, A.K. Two-dimensional gas of massless Dirac fermions in graphene. *Nature* **2005**, *438*, 192–200. [[CrossRef](#)] [[PubMed](#)]
- Do, V.N.; Pham, T.H. Graphene and its one-dimensional patterns: From basic properties towards applications. *Adv. Nat. Sci. Nanosci. Nanotechnol.* **2010**, *1*, 033001. [[CrossRef](#)]
- Wintterlin, J.; Bocquet, M.-L. Graphene on metal surfaces. *Surf. Sci.* **2009**, *603*, 1841–1852. [[CrossRef](#)]
- Lebègue, S.; Eriksson, O. Electronic structure of two-dimensional crystals from ab initio theory. *Phys. Rev. B* **2009**, *79*, 115409. [[CrossRef](#)]
- Nicolosi, V.; Chhowalla, M.; Kanatzidis, M.G.; Strano, M.S.; Coleman, J.N. Liquid Exfoliation of Layered Materials. *Science* **2013**, *340*, 1226419. [[CrossRef](#)]
- Radisavljevic, B.; Radenovic, A.; Brivio, J.; Giacometti, V.; Kis, A. Single-layer MoS₂ transistors. *Nat. Nanotech.* **2011**, *6*, 147–150. [[CrossRef](#)] [[PubMed](#)]
- Mak, K.F.; Lee, C.; Hone, J.; Shan, J.; Heinz, T.F. Atomically Thin MoS₂: A New Direct-Gap Semiconductor. *Phys. Rev. Lett.* **2010**, *105*, 136805. [[CrossRef](#)] [[PubMed](#)]
- Splendiani, A.; Sun, L.; Zhang, Y.; Li, T.; Mak, J.; Chim, C.-Y.; Galli, G.; Wang, F. Emerging photoluminescence in monolayer MoS₂. *Nano Lett.* **2010**, *10*, 1271–1275. [[CrossRef](#)] [[PubMed](#)]
- Eknapakul, T.; King, P.D.; Lombardo, A.; Krupke, R.; Ferrari, A.C.; Avouris, P.; Steiner, M. Electronic structure of a quasi-freestanding MoS₂ monolayer. *Nano Lett.* **2014**, *14*, 1312–1316. [[CrossRef](#)] [[PubMed](#)]
- Cheiwchanchamnangij, T.; Lambrecht, W.R.L. Quasiparticle band structure calculation of monolayer, bilayer, and bulk MoS₂. *Phys. Rev. B* **2012**, *85*, 205302. [[CrossRef](#)]
- Yakovkin, I.N. Interlayer interaction and screening in MoS₂. *Surf. Rev. Lett.* **2014**, *21*, 1450039. [[CrossRef](#)]
- Ye, M.; Winslow, D.; Zhang, D.; Pandey, R.; Yap, Y.K. Recent Advancement on the Optical Properties of Two-Dimensional Molybdenum Disulfide (MoS₂) Thin Films. *Photonics* **2015**, *2*, 288–307. [[CrossRef](#)]
- Hedin, L. New Method for Calculating the One-Particle Green's Function with Application to the Electron-Gas Problem. *Phys. Rev.* **1965**, *139*, A796. [[CrossRef](#)]
- Enderlein, C.; Kim, Y.S.; Bostwick, A.; Rotenberg, E.; Horn, K. The formation of an energy gap in graphene on ruthenium by controlling the interface. *New J. Phys.* **2010**, *12*, 033014. [[CrossRef](#)]
- Giovannetti, G.; Khomyakov, P.A.; Brocks, G.; Karpan, V.M.; van den Brink, J.; Kelly, P.J. Doping graphene with metal contacts. *Phys. Rev. Lett.* **2008**, *101*, 026803. [[CrossRef](#)] [[PubMed](#)]
- Bostwick, A.; Ohta, T.; McChesney, J.L.; Emtsev, K.V.; Seyller, T.; Horn, K.; Rotenberg, E. Symmetry breaking in few layer graphene films. *New J. Phys.* **2007**, *9*, 385. [[CrossRef](#)]
- Ohta, T.; Bostwick, A.; Seyller, T.; Horn, K.; Rotenberg, E. Controlling the electronic structure of bilayer graphene. *Science* **2006**, *313*, 951–954. [[CrossRef](#)] [[PubMed](#)]
- Zhou, S.Y.; Gweon, G.H.; Fedorov, A.V.; First, P.N.; de Heer, W.A.; Lee, D.H.; Guinea, F.; Castro Neto, A.H.; Lanzara, A. Substrate-induced bandgap opening in epitaxial graphene. *Nat. Mater.* **2007**, *6*, 770–775.
- Skomski, R.; Dowben, P.A.; Sky Driver, M.; Kelber, J.A. Sublattice-induced symmetry breaking and bandgap formation in grapheme. *Mater. Horiz.* **2014**. [[CrossRef](#)]
- Kumar, P.; Skomski, R.; Manchanda, P.; Kashyap, A.; Dowben, P.A. Effective mass and band gap of strained graphene. *Curr. Appl. Phys.* **2014**, *14*, S136. [[CrossRef](#)]
- Nakada, K.; Fujita, M.; Dresselhaus, G.; Dresselhaus, M.S. Edge state in graphene ribbons: Nanometer size effect and edge shape dependence. *Phys. Rev. B* **1996**, *54*, 17954. [[CrossRef](#)]

26. Yin, W.-J.; Xie, Y.-E.; Liu, L.-M.; Wang, R.-Z.; Wei, X.-L.; Lau, L.; Zhong, J.-X.; Chen, Y.-P. R-graphyne: A new two-dimensional carbon allotrope with versatile Dirac-like point in nanoribbons. *J. Mater. Chem. A* **2013**, *1*, 5341–5346. [[CrossRef](#)]
27. Pivetta, M.; Patthey, F.; Barke, I.; Hovel, H.; Delley, B.; Schneider, W.-D. Gap opening in the surface electronic structure of graphite induced by adsorption of alkali atoms: Photoemission experiments and density functional calculations. *Phys. Rev. B* **2005**, *71*, 165430. [[CrossRef](#)]
28. Petrova, N.V.; Yakovkin, I.N. DFT calculations of the electronic structure and interlayer interaction in the Li-intercalated graphene bilayer. *Surf. Rev. Lett.* **2016**, *24*, 1750020. [[CrossRef](#)]
29. Sutter, P.W.; Flege, J.-I.; Sutter, E.A. Epitaxial graphene on ruthenium. *Nat. Mater.* **2008**, *7*, 406–411. [[CrossRef](#)] [[PubMed](#)]
30. Jiang, D.-E.; Du, M.-H.; Dai, S. First principles study of the graphene/Ru(0001) interface. *J. Chem. Phys.* **2009**, *130*, 074705. [[CrossRef](#)] [[PubMed](#)]
31. Yakovkin, I.N. Band structure of Au layers on the Ru(0001) and graphene/Ru(0001) surfaces. *Eur. Phys. J. B* **2012**, *85*, 61. [[CrossRef](#)]
32. Varykhalov, A.; Sanchez-Barriga, J.; Shikin, A.M.; Biswas, C.; Vescovo, E.; Rybkin, A.; Marchenko, D.; Rader, O. Electronic and magnetic properties of quasifreestanding graphene on Ni. *Phys. Rev. Lett.* **2008**, *101*, 157601. [[CrossRef](#)] [[PubMed](#)]
33. Pletikosić, I.; Kralj, M.; Pervan, P.; Brako, R.; Coraux, J.; N'Diaye, A.T.; Busse, C.; Michely, T. Dirac Cones and Minigaps for Graphene on Ir(111). *Phys. Rev. Lett.* **2009**, *102*, 056808. [[CrossRef](#)] [[PubMed](#)]
34. Di Sante, D.; Stroppa, A.; Barone, P.; Whangbo, M.-H.; Picozzi, S. Emergence of ferroelectricity and spin-valley properties in two-dimensional honeycomb binary compounds. *Phys. Rev. B* **2015**, *91*, 161401(R). [[CrossRef](#)]
35. Peierls, R.E. *Quantum Theory of Solids*; Clarendon Press: Oxford, UK, 1955.
36. Mermin, N.D. Crystalline Order in Two Dimensions. *Phys. Rev.* **1968**, *176*, 250–254. [[CrossRef](#)]
37. Lee, S.-H.; Chung, H.-J.; Heo, J.; Yang, H.; Shin, J.; Chung, U.-I.; Seo, S. Band Gap Opening by Two-Dimensional Manifestation of Peierls Instability in Graphene. *ACS Nano* **2011**, *5*, 2964–2969. [[CrossRef](#)] [[PubMed](#)]
38. Son, Y.-W.; Cohen, M.L.; Louie, S.G. Energy Gaps in Graphene Nanoribbons. *Phys. Rev. Lett.* **2006**, *97*, 216803. [[CrossRef](#)] [[PubMed](#)]
39. Abanin, D.A.; Shytov, A.V.; Levitov, L.S. Peierls-Type Instability and Tunable Band Gap in Functionalized Graphene. *Phys. Rev. Lett.* **2010**, *105*, 086802. [[CrossRef](#)] [[PubMed](#)]
40. Batra, I.P. Gapless Peierls transition. *Phys. Rev. B* **1990**, *42*, 9162–9165. [[CrossRef](#)]
41. Yakovkin, I.N. Atomic wires. In *Encyclopedia of Nanoscience and Nanotechnology*; Nalwa, H.S., Ed.; American Scientific Publishers: Valencia, CA, USA, 2004; Volume 1, pp. 169–190.
42. Yakovkin, I.N. Metallicity of atomic wires. *Appl. Surf. Sci.* **2006**, *252*, 6127–6134. [[CrossRef](#)]
43. Bostwick, A.; McChesney, J.L.; Emtsev, K.V.; Seyller, T.; Horn, K.; Kevan, S.D.; Rotenberg, E. Quasiparticle transformation during a metal insulator transition in graphene. *Phys. Rev. Lett.* **2009**, *103*, 056404. [[CrossRef](#)] [[PubMed](#)]
44. Park, C.-H.; Giustino, F.; Spataru, C.D.; Cohen, M.L.; Louie, S.G. First-principles study of electron linewidths in graphene. *Phys. Rev. Lett.* **2009**, *102*, 0768034. [[CrossRef](#)] [[PubMed](#)]
45. Kim, S.; Ihm, J.; Choi, H.J.; Son, Y.-W. Origin of anomalous electronic structures of epitaxial graphene on silicon carbide. *Phys. Rev. Lett.* **2008**, *100*, 1768024. [[CrossRef](#)] [[PubMed](#)]
46. Lennard-Jones, J.E. Processes of adsorption and diffusion on solid surfaces. *Trans. Faraday Soc.* **1932**, *28*, 333–359. [[CrossRef](#)]
47. London, F. The general theory of molecular forces. *Trans. Faraday Soc.* **1937**, *33*, 8–26. [[CrossRef](#)]
48. Stone, A.J. *The Theory of Intermolecular Forces*; Clarendon Press: Oxford, UK, 1996.
49. Berland, K.; Cooper, V.R.; Lee, K.; Schröder, E.; Thonhauser, T.; Hyldgaard, P.; Lundqvist, B.I. Van der Waals forces in density functional theory: A review of the vdW-DF method. *Rep. Prog. Phys.* **2015**, *78*, 066501. [[CrossRef](#)] [[PubMed](#)]
50. Grimme, S. Density functional theory with London dispersion corrections. *WIREs Comput. Mol. Sci.* **2011**, *1*, 211–228. [[CrossRef](#)]
51. Tkatchenko, A.; Romaner, L.; Hofmann, O.T.; Zojer, E.; Ambrosch-Draxl, C.; Scheffler, M. Van der Waals interactions between organic adsorbates and at organic/inorganic interfaces. *MRS Bull.* **2010**, *35*, 435–442. [[CrossRef](#)]

52. Klimeš, J.; Michaelides, A. Perspective: Advances and challenges in treating van der Waals dispersion forces in density functional theory. *J. Chem. Phys.* **2012**, *137*, 120901. [[CrossRef](#)] [[PubMed](#)]
53. Andersson, Y.; Langreth, D.C.; Lundqvist, B.I. van der Waals Interactions in Density-Functional Theory. *Phys. Rev. Lett.* **1996**, *76*, 102. [[CrossRef](#)] [[PubMed](#)]
54. Dion, M.; Rydberg, H.; Schröder, E.; Langreth, D.C.; Lundqvist, B.I. Van der Waals Density Functional for General Geometries. *Phys. Rev. Lett.* **2004**, *92*, 246401. [[CrossRef](#)] [[PubMed](#)]
55. Thonhauser, T.; Cooper, V.R.; Li, S.; Puzder, A.; Hyldgaard, P.; Langreth, D.C. Van der Waals density functional: Self-consistent potential and the nature of the van der Waals bond. *Phys. Rev. B* **2007**, *76*, 125112. [[CrossRef](#)]
56. Reilly, A.M.; Tkatchenko, A. Understanding the role of vibrations, exact exchange, and many-body van der Waals interactions in the cohesive properties of molecular crystals. *J. Chem. Phys.* **2013**, *139*, 024705. [[CrossRef](#)] [[PubMed](#)]
57. Silvestrelli, P.L.; Ambrosetti, A. Including screening in van der Waals corrected density functional theory calculations: The case of atoms and small molecules physisorbed on graphene. *J. Chem. Phys.* **2014**, *140*, 124107. [[CrossRef](#)] [[PubMed](#)]
58. Brako, R.; Sokcević, D.; Lazić, P.; Atodiresei, N. Graphene on the Ir(111) surface: From van der Waals to strong bonding. *New J. Phys.* **2010**, *12*, 113016. [[CrossRef](#)]
59. Khomyakov, P.A.; Giovannetti, G.; Rusu, P.C.; Brocks, G.; van den Brink, J.; Kelly, P.J. First-principles study of the interaction and charge transfer between graphene and metals. *Phys. Rev. B* **2009**, *79*, 195425. [[CrossRef](#)]
60. Feibelman, P.J. DFT Versus the “Real World” (or, Waiting for Godft). *Top. Catal.* **2010**, *53*, 417–422. [[CrossRef](#)]
61. Shulenburg, L.; Baczewski, A.D.; Zhu, Z.; Guan, J.; Tomanek, D. The Nature of the Interlayer Interaction in Bulk and Few-Layer Phosphorus. *Nano Lett.* **2015**, *15*, 8170–8175. [[CrossRef](#)] [[PubMed](#)]
62. Yakovkin, I.N.; Petrova, N.V. Hydrogen-induced metallicity and strengthening of MoS₂. *Chem. Phys.* **2014**, *434*, 20–24. [[CrossRef](#)]
63. Petrova, N.V.; Yakovkin, I.N.; Zeze, D.A. Metallization and stiffness of the Li-intercalated MoS₂ bilayer. *Appl. Surf. Sci.* **2015**, *353*, 333–337. [[CrossRef](#)]
64. Yakovkin, I.N. Band structure of the MoS₂ bilayer with adsorbed and intercalated Na. *Phys. Status Solidi B* **2015**, *252*, 2693–2697. [[CrossRef](#)]
65. LaShell, S.; McDougall, B.A.; Jensen, E. Spin Splitting of an Au(111) Surface State Band Observed with Angle Resolved Photoelectron Spectroscopy. *Phys. Rev. Lett.* **1996**, *77*, 3419. [[CrossRef](#)] [[PubMed](#)]
66. Koroteev, Y.M.; Bihlmayer, G.; Gayone, J.E.; Chulkov, E.V.; Blügel, S.; Echenique, P.M.; Hofmann, P. Strong Spin-Orbit Splitting on Bi Surfaces. *Phys. Rev. Lett.* **2004**, *93*, 046403. [[CrossRef](#)] [[PubMed](#)]
67. Bychkov, Y.A.; Rashba, E.I. Properties of a 2D electron gas with lifted spectral degeneracy. *JETP Lett.* **1984**, *39*, 78.
68. Bihlmayer, G.; Koroteev, Y.M.; Echenique, P.M.; Chulkov, E.V.; Blügel, S. The Rashba-effect at metallic surfaces. *Surf. Sci.* **2006**, *600*, 3888–3891. [[CrossRef](#)]
69. Zhu, Z.Y.; Cheng, Y.C.; Schwingenschlög, U. Giant spin-orbit-induced spin splitting in two-dimensional transition-metal dichalcogenide semiconductors. *Phys. Rev. B* **2011**, *84*, 153402. [[CrossRef](#)]
70. Kobayashi, K.; Yamauchi, J. Electronic structure and scanning-tunneling-microscopy image of molybdenum dichalcogenide surfaces. *Phys. Rev. B Condens. Matt.* **1995**, *51*, 17085–17095. [[CrossRef](#)]
71. Jin, W.; Yeh, P.-C.; Zaki, N.; Zhang, D.; Sadowski, J.T.; Al-Mahboob, A.; van der Zande, A.M.; Chenet, D.A.; Dadap, J.I.; Herman, I.P. Direct Measurement of the Thickness-Dependent Electronic Band Structure of MoS₂ Using Angle-Resolved Photoemission Spectroscopy. *Phys. Rev. Lett.* **2013**, *111*, 106801. [[CrossRef](#)] [[PubMed](#)]
72. Yakovkin, I.N.; Dowben, P.A. The problem of the band gap in LDA calculations. *Surf. Rev. Lett.* **2007**, *14*, 481–487. [[CrossRef](#)]
73. Kleinman, L.; Lee, S. Gradient expansion of the exchange-energy density functional: Effect of taking limits in the wrong order. *Phys. Rev. B* **1988**, *37*, 4634. [[CrossRef](#)]
74. Perdew, J.P.; Burke, K.; Ernzerhof, M. Generalized Gradient Approximation Made Simple. *Phys. Rev. Lett.* **1996**, *77*, 3865. [[CrossRef](#)] [[PubMed](#)]
75. Yakovkin, I.N.; Petrova, N.V. Influence of the thickness and surface composition on the electronic structure of FeS₂ layers. *Appl. Surf. Sci.* **2016**, *377*, 184–190. [[CrossRef](#)]
76. Alonso, J.A.; Girifalco, L.A. Nonlocal approximation to the exchange potential and kinetic energy of an inhomogeneous electron gas. *Phys. Rev.* **1978**, *17*, 3735. [[CrossRef](#)]

77. Gunnarsson, O.; Jonson, M.; Lundqvist, B.I. Descriptions of exchange and correlation effects in inhomogeneous electron systems. *Phys. Rev. B* **1979**, *20*, 3136. [[CrossRef](#)]
78. Ramasubramaniam, A. Large excitonic effects in monolayers of molybdenum and tungsten dichalcogenides. *Phys. Rev. B* **2012**, *86*, 115409. [[CrossRef](#)]
79. Qiu, D.Y.; da Jornada, F.H.; Louie, S.G. Optical spectrum of MoS₂: Many-body effects and diversity of exciton states. *Phys. Rev. Lett.* **2013**, *111*, 216805. [[CrossRef](#)] [[PubMed](#)]
80. Ugeda, M.M.; Bradley, A.J.; Shi, S.-F.; da Jornada, F.H.; Zhang, Y.; Qiu, D.Y.; Ruan, W.; Mo, S.-K.; Hussain, Z.; Shen, Z.-X.; et al. Observation of giant bandgap renormalization and excitonic effects in a monolayer transition metal dichalcogenide semiconductor. *Nat. Mater* **2014**, *13*, 1091–1095. [[CrossRef](#)] [[PubMed](#)]
81. Bradley, A.J.; Ugeda, M.M.; da Jornada, F.H.; Qiu, D.Y.; Ruan, W.; Zhang, Y.; Wickenburg, A.; Riss, S.; Lu, J.; Mo, S.-K.; et al. Probing the Role of Interlayer Coupling and Coulomb Interactions on Electronic Structure in Few-Layer MoSe₂ Nanostructures. *Nano Lett.* **2015**, *15*, 2594–2599. [[CrossRef](#)] [[PubMed](#)]
82. Pelant, I.; Valenta, J. *Luminescence Spectroscopy of Semiconductors*; Oxford University Press: Oxford, UK, 2012.
83. Mak, K.F.; He, K.; Lee, C.; Lee, G.H.; Hone, J.; Heinz, T.F.; Shan, J. Tightly bound trions in monolayer MoS₂. *Nat. Mater.* **2013**, *12*, 207–211. [[CrossRef](#)] [[PubMed](#)]
84. Huard, V.; Cox, R.T.; Saminadayar, K.; Arnoult, A.; Tatarenko, S. Bound states in optical absorption of semiconductor quantum wells containing a two-dimensional electron gas. *Phys. Rev. Lett.* **2000**, *84*, 187–190. [[CrossRef](#)] [[PubMed](#)]
85. Komsa, H.-P.; Krasheninnikov, A.V. Effects of confinement and environment on the electronic structure and exciton binding energy of MoS₂ from first principles. *Phys. Rev. B* **2012**, *86*, 241201(R). [[CrossRef](#)]
86. Calman, E.V.; Dorow, C.J.; Fogler, M.M.; Butov, L.V.; Hu, S.; Mishchenko, A.; Geim, A.K. Control of excitons in multi-layer van der Waals heterostructures. *Appl. Phys. Lett.* **2016**, *108*, 101901. [[CrossRef](#)]
87. Dileep, K.; Sahu, R.; Sarkar, S.; Peter, S.C.; Datta, R. Layer specific optical band gap measurement at nanoscale in MoS₂ and ReS₂ van der Waals compounds by high resolution electron energy loss spectroscopy. *J. Appl. Phys.* **2016**, *119*, 114309. [[CrossRef](#)]
88. Zhang, C.; Johnson, A.; Hsu, C.L.; Li, L.J.; Shih, C.K. Direct Imaging of Band Profile in Single Layer MoS₂ on Graphite: Quasiparticle Energy Gap, Metallic Edge States, and Edge Band Bending. *Nano Lett.* **2014**, *14*, 2443–2447. [[CrossRef](#)] [[PubMed](#)]
89. Ulstrup, S.; Čabo, A.G.; Miwa, J.A.; Riley, J.M.; Grønborg, S.S.; Johannsen, J.C.; Cacho, C.; Alexander, O.; Chapman, R.T.; Springate, E.; et al. Ultrafast Band Structure Control of a Two-Dimensional Heterostructure. *ACS Nano* **2016**, *10*, 6315–6322. [[CrossRef](#)] [[PubMed](#)]
90. Aziza, Z.B.; Henck, H.; Felice, D.; Di Pierucci, D.; Chaste, J.; Naylor, C.H.; Balan, A.; Dappe, Y.J.; Johnson, A.T.C.; Ouerghi, A. Bandgap inhomogeneity of MoS₂ monolayer on epitaxial graphene bilayer in van der Waals p-n junction. *Carbon* **2016**, *110*, 396–403. [[CrossRef](#)]
91. Jin, W.; Yeh, P.-C.; Zaki, N.; Chenet, D.; Arefe, G.; Hao, Y.; Sala, A.; Mentis, T.O.; Dadap, J.I.; Locatelli, A.; et al. Tuning the electronic structure of monolayer graphene/MoS₂ van der Waals heterostructures via interlayer twist. *Phys. Rev. B* **2015**, *92*, 201409(R). [[CrossRef](#)]
92. Diaz, H.C.; Avila, J.; Chen, C.; Addou, R.; Asensio, M.C.; Batzill, M. Direct Observation of Interlayer Hybridization and Dirac Relativistic Carriers in Graphene/MoS₂ van der Waals Heterostructures. *Nano Lett.* **2015**, *15*, 1135–1140. [[CrossRef](#)] [[PubMed](#)]
93. Pierucci, D.; Henck, H.; Avila, J.; Balan, A.; Naylor, C.H.; Patriarcho, G.; Dappe, Y.J.; Silly, M.G.; Sirotti, F.; Johnson, A.T.C.; et al. Band Alignment and Minigaps in Monolayer MoS₂—Graphene van der Waals Heterostructures. *Nano Lett.* **2016**, *16*, 4054–4061. [[CrossRef](#)] [[PubMed](#)]

